# Spatial structure of low-frequency fluctuations throughout the transition of poloidal flow velocity in edge plasmas of LHD



# Spatial structure of low-frequency fluctuations throughout the transition of poloidal flow velocity in edge plasmas of LHD

Cite as: Phys. Plasmas **26**, 092302 (2019); https://doi.org/10.1063/1.5098954
Submitted: 04 April 2019 • Accepted: 22 August 2019 • Published Online: 18 September 2019

C. Moon, T. Kobayashi, K. Ida, et al.

Physics of Plasmas ARTICLE scitation.org/journal/php

# Spatial structure of low-frequency fluctuations throughout the transition of poloidal flow velocity in edge plasmas of LHD

Cite as: Phys. Plasmas **26**, 092302 (2019); doi: 10.1063/1.5098954
Submitted: 4 April 2019 · Accepted: 22 August 2019 ·
Published Online: 17 September 2019



C. Moon,[1,2,a)] T. Kobayashi,[2] K. Ida,[2] T. Tokuzawa,[2] C. Hidalgo,[3] M. Yoshinuma,[2] K. Ogawa,[2] K. Itoh,[4] A. Fujisawa,[1] and LHD Experiment Group[2,b)]

## AFFILIATIONS

[1]Research Institute for Applied Mechanics and Research Center for Plasma Turbulence, Kyushu University, 6-1 Kasuga-Koen, Kasuga 816-8580, Japan
[2]National Institute for Fusion Science, National Institutes of Natural Sciences, 322-6 Oroshi-cho, Toki, Gifu 509-5292, Japan
[3]Laboratorio Nacional de Fusión, Asociación EURATOM-CIEMAT, 28040 Madrid, Spain
[4]Institute of Science and Technology Research, Chubu University, Kasugai, Aichi 487-8501, Japan

[a)]Electronic mail: moon@riam.kyushu-u.ac.jp
[b)]http://www.nifs.ac.jp/en/research/index.html

## ABSTRACT

It is observed that a low-frequency (∼2 kHz) density fluctuation is excited in a transition of the poloidal flow velocity ($V_\theta$) in the edge magnetic stochastic region of the Large Helical Device plasmas. Furthermore, it is found that the propagation velocity becomes approximately zero in the proximity of the appearance region of the low-frequency fluctuation by using the edge multichannel microwave Doppler reflectometer system. In particular, the low-frequency fluctuation is considered to be transmitted in both directions (inward and outward) away from the excitation position of the fluctuation, which behaves as the precursor of a magnetic fluctuation burst. Afterward, the edge $H_\alpha$ signal intensity is sharply increased.



## I. INTRODUCTION

A more comprehensive understanding of the magneto-hydrodynamics (MHD) in the magnetically confined plasmas[1] is crucially important for achieving the steady state nuclear fusion reactor. In helical systems, it is widely accepted that core and edge magnetic stochastic regions exist,[2,3] which can degrade global plasma confinement. Moreover, in the edge magnetic stochastic region of the helical systems, many small magnetic islands exist[3] which interact with edge plasma turbulence (or with each other), enhancing magnetic activity. On the other hand, MHD fluctuations are not observed easily in the edge magnetic stochastic regions, whereas the global MHD fluctuations are observed in the low-order rational surfaces.[8–11] In addition, the edge radial electric field ($E_r$) corresponding to the poloidal flow velocity ($V_\theta$) structure is directly related to the topology and the structure of the edge magnetic field in the magnetically confined plasmas.[12,13]

Recently, the neoclassical viscosity has been interpreted as the restoring force which drives the system back to ambipolarity and vanishes at the critical density (at the transition from the electron to the ion neoclassical root). This allows large deviations of $E_r$ from the neoclassical ambipolarity including the amplification of (low-frequency fluctuations) zonal flows. This first principles theoretical prediction has been validated in the TJ-II stellarator.[14] However, there has been no experimental study to examine the effect of the transition $E_r$ on a low-frequency fluctuation in the edge plasmas of helical systems. Therefore, a study of the response of the low-frequency fluctuations in the transition of $E_r$ in the edge stochastic magnetic region is an important issue for understanding the edge plasma dynamics.

In this paper, we investigated the spatiotemporal structure of a low-frequency fluctuation in edge plasmas, which emerges at the transition of $V_\theta$ (which is roughly identical with the $E_r$) of Large Helical Device (LHD).[15] For the stellarator geometry physics, there is no large toroidal rotation because of the parallel viscosity in the toroidal direction;[16] hence, $E_r$ is mainly determined by the poloidal flow velocity $V_\theta$. Furthermore, the microwave Doppler reflectometer system is the most

suitable for measuring the specific local density fluctuations.[17–30] For this reason, the low-frequency fluctuation is investigated by using the multichannel microwave Doppler reflectometer system in order to discuss the interplay between the $V_\theta$ structural transition and the fluctuation specifically in the edge plasmas. These results will provide a better understanding of the dynamical response of plasma fluctuation at the transition of $V_\theta$ in the edge stochastic magnetic region.

## II. TIME EVOLUTION OF PLASMA PARAMETERS

The LHD is a superconducting stellarator with a major radius $R = 3.6$ m and a minor radius $a = 0.6$ m; the vacuum magnetic configuration can be controlled by the preset vacuum magnetic axis position, $R_{ax}$. Figure 1 shows a Poincaré plot of the vacuum magnetic field lines for $R_{ax} = 3.6$ m, where the reflectometer and $r_{eff}$ indicate the channel numbers of the microwave Doppler reflectometer system and the averaged minor radius on the magnetic flux surface, respectively. Figure 2 shows the characteristic plasma parameters for the target discharge (#118187), which are initially produced by the electron cyclotron heating (ECH) and sustained with two perpendicular neutral beam injection (NBI) systems. The power of the ECH and the perpendicular NBIs are approximately 1 MW and 5 MW, respectively. In addition, the codirection tangential NBI (~4 MW) and counterdirection tangential NBI (~5 MW) are injected at $t \simeq 4.0$ s, as shown in Fig. 2(a). The power of the tangential NBIs is the injected power, and the codirection and counterdirection refer to the directions that are in the same and opposite directions to the toroidal plasma current. The working gas is hydrogen, and the magnetic configuration with the toroidal magnetic field strength of $B_T = -2.75$ T at the $R_{ax} = 3.6$ m is used.

The profiles of the electron temperature ($T_e$) and the density ($n_e$) are measured by the Thomson scattering diagnostic (YAG laser).[31] The profiles of the ion temperature ($T_i$) and the poloidal flow velocity $V_\theta$ are measured by the charge exchange spectroscopy (CXS).[32,33] The fully ionized carbon is measured with CXS using the NBI for the $T_i$ and $V_\theta$ measurements. The highest radial resolution of the CXS measurement is approximately 9 mm. The perpendicular flow velocity ($V_\perp$) is measured by the Doppler reflectometer. After the tangential NBIs are injected, the central $T_e$ and $T_i$ are significantly increased, but the central $n_e$ remains almost constant in $4.0\ \text{s} < t < 4.12$ s. In particular, a transition of the edge $V_\theta$ ($V_\theta$ begins to change from negative value to positive value) occurs by injecting the tangential NBIs in $4.0\ \text{s} < t < 4.12$ s. Furthermore, a transition of the edge $V_\perp$ also occurs around the time of $V_\theta$ transition. In these experimental conditions, $V_\theta$ corresponds to $E_r$, since the contribution of the toroidal flow velocity to $E_r$ is much smaller than that of the poloidal flow velocity $V_\theta$.[32,34]

Figure 3 shows the radial profiles of (a) the electron temperature ($T_e$), (b) the ion temperature ($T_i$), (c) the electron density ($n_e$), and (d) the poloidal flow velocity ($V_\theta$) for $t \simeq 4.04$ s (blue circles) and 4.13 s (red circles). The location of the vacuum last closed flux surface

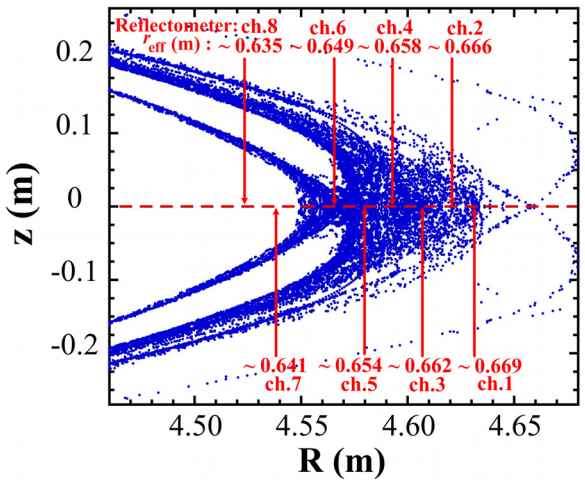


**FIG. 1.** The Poincaré plot of the vacuum magnetic field lines ($R_{ax} = 3.6$ m) plotted at the horizontal elongated cross section. The red solid arrows indicate the channel numbers of the microwave Doppler reflectometer system corresponding to the averaged minor radius ($r_{eff}$).

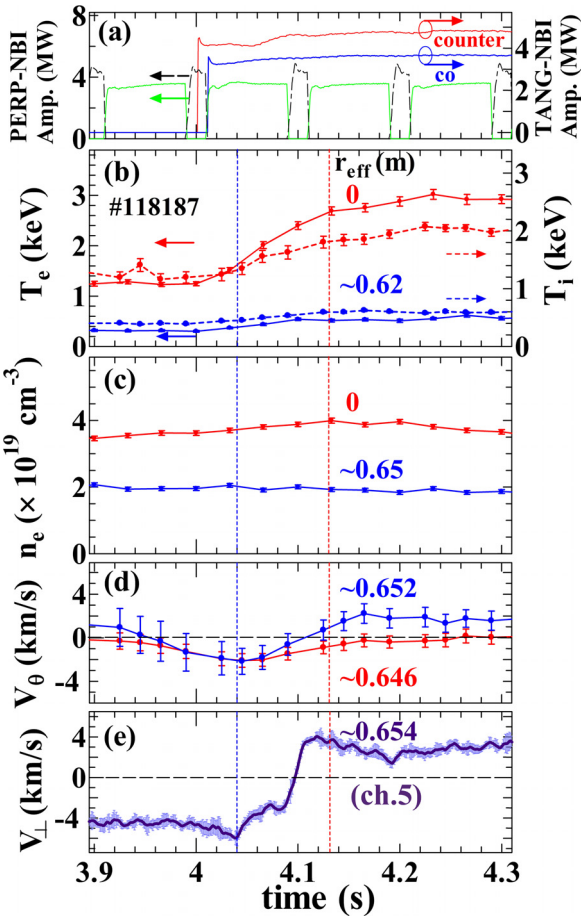


**FIG. 2.** Time evolution of (a) the NBI powers; the black and the green indicate the perpendicular direction, and the blue (coinjection) and the red (counterinjection) indicate the tangential direction, (b) the electron temperatures ($T_e$) and the ion temperatures ($T_i$), (c) the electron density ($n_e$), (d) the poloidal flow velocity ($V_\theta$), and (e) the perpendicular flow velocity ($V_\perp$) in the LHD. Both $T_e$ and $n_e$ profiles are measured by the Thomson scattering diagnostic (YAG laser). $T_i$ and $V_\theta$ are measured with the charge exchange spectroscopy (CXS). $V_\perp$ is measured by the Doppler reflectometer system.

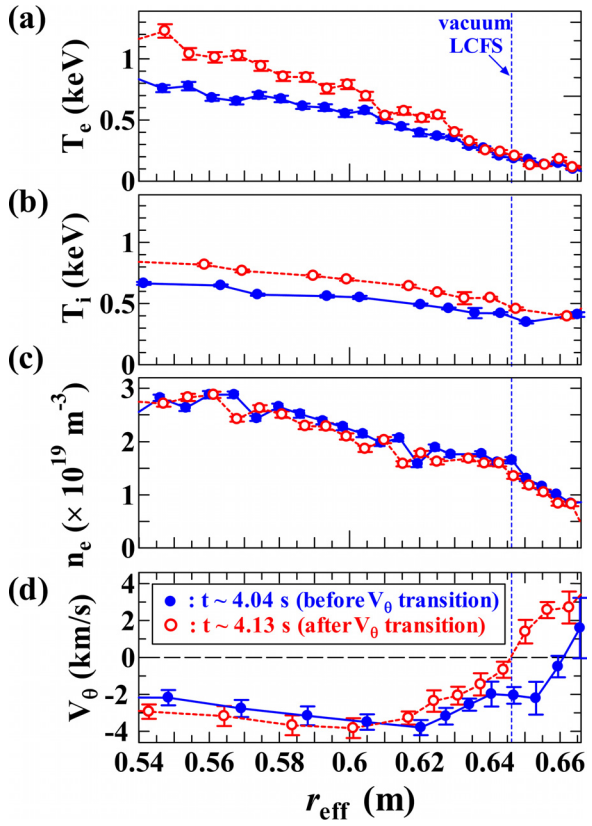


**FIG. 3.** Radial profiles of (a) the electron temperature ($T_e$), (b) the ion temperature ($T_i$), (c) the electron density ($n_e$), and (d) the poloidal flow velocity ($V_\theta$) for $t \simeq 4.04$ s (blue circles: before the $V_\theta$ transition) and 4.13 s (red circles: after the $V_\theta$ transition). The blue dotted line indicates the vacuum last closed flux surface (LCFS).

(LCFS) is $r_{eff} \simeq 0.64$ m. It should be noted that even though the location of the effective LCFS is still under debate,[13,35] the location of the transition is a little away from the LCFS, which corresponds to the edge magnetic stochastic regions of LHD (see Fig. 1). In addition, the ion temperature profile is changed during the transition of $V_\theta$, while the electron temperature and the density profiles are not changed in the edge magnetic stochastic regions of LHD.

## III. OBSERVATION OF THE TRANSIENT LOW-FREQUENCY FLUCTUATIONS

### A. Low-frequency fluctuations in the edge plasmas

The plasma fluctuations during the transition in the edge LHD plasma are investigated in detail by means of the wavelet spectral analysis. The spatial measurement points of the multichannel microwave Doppler reflectometer systems are almost fixed, since the density profile remains constant during the transition. In order to determine the proper cutoff positions of the Doppler reflectometer, the cutoff layer based on the cutoff plasma density is calculated by comparing the CXS with the Doppler reflectometer system data to the radial positions for the same propagation velocity formation.[36] Namely, this procedure is used to associate the reflectometer channels to radial positions through comparison with the CXS measurements. In addition, it is confirmed that the ambiguity of the cutoff layer is less than 30% in comparison with the cutoff layer based on the equilibrium density profile (which is calculated by the Thomson Scattering diagnostics). Here, the O-mode eight launching frequencies of the Doppler reflectometer system are 27.7, 29.0, 30.5, 32.0, 33.3, 34.8, 37.0, and 38.3 GHz corresponding to approximately the radial positions ($r_{eff}$) 0.669, 0.666, 0.662, 0.658, 0.654, 0.649, 0.641, and 0.635 m, respectively. Note that the measurement uncertainty on the radial position of the reflectometer channels is approximately 0.01 m in the edge LHD plasmas.[39]

Figure 4(a) shows the time evolution of $H_\alpha$ signal and the local perpendicular flow velocity measured with the Doppler reflectometer channel at $r_{eff} \simeq 0.654$ m (the ch.5 is thought to be associated with the excitation position for the low-frequency fluctuation). It is observed that the sign of $V_\perp$ changes from minus value to plus value, i.e., from ion diamagnetic direction to electron diamagnetic direction. Furthermore, the value of $V_\perp$ crosses the centerline ($V_\perp \simeq 0$ km/s) at $t \simeq 4.097$ s and afterward $H_\alpha$ signal shows a tiny increase, which indicates a small plasma density and/or energy loss at $t \simeq 4.102$ s. Figures 4(b) and 4(c) show the wavelet power spectra of $H_\alpha$ signal and the magnetic probe signal (detecting $\sim B_\theta$), respectively. In the low-frequency regime, in Figs. 4(d)–4(f), a transient chirping up density fluctuation is detected (see the black eye-guide). First of all, in Fig. 4(g), a density fluctuation with $f \simeq 1$ kHz emerges at $t \simeq 4.091$ s, where $V_\perp$ becomes approximately zero for $r_{eff} \simeq 0.658$ m. As time passes, in Figs. 4(d)–4(f), the frequency of fluctuation increases up to $f \simeq 4$ kHz, and the fluctuation amplitude seems to be enhanced. Finally, the low-frequency fluctuation suddenly disappears, likely leading to an increase in the $H_\alpha$ signal intensity. We attempted to obtain the poloidal mode structure of the fluctuation by analyzing the phase difference of the poloidal magnetic probe array data.[37] The main component of the mode is $m \sim 2$. Note that the coherence of signals is relatively low because of the burst feature of the low-frequency fluctuation, and the fluctuation consists of the higher poloidal mode numbers. Furthermore, the frequency chirping of $\Delta f \simeq 3$ kHz is the same order of the Doppler shift frequency as from the local $E_r$ ($\sim V_\perp$) at the transition time.

### B. Spatial structure of the low-frequency fluctuations

The 8-channel Doppler reflectometer system data are analyzed in order to investigate the spatial structure of the low-frequency fluctuations. Figures 4(d)–4(g) show the wavelet power spectra of the density fluctuations measured with the four outer channels of the Doppler reflectometer at $r_{eff} \simeq 0.669$ m, $r_{eff} \simeq 0.666$ m, $r_{eff} \simeq 0.662$ m, and $r_{eff} \simeq 0.658$ m, respectively. It is shown that the chirping up fluctuation appears in edge plasmas of LHD. Note that the signal is independently normalized in each channel, although the relative calibration of the fluctuation intensity has not been performed. The other four inner channels do not detect those fluctuations clearly.

Figure 5 shows the integrated fluctuations power spectra in order to analyze the spatial structure of the bursty magnetic [Fig. 5(a)] and density [Figs. 5(b)–5(e)] fluctuations; the wavelet power spectra are integrated in $\sim 1$ kHz $< f < \sim 3$ kHz. It is found that the peak of the fluctuation envelope moves outward, and the propagation velocity of the fluctuation envelope is estimated to be approximately $V_r \sim 2$ m/s by using the Doppler reflectometer system data.

Figure 6 shows the contours of the cross correlation function of the Doppler reflectometer system channels with the reference channel

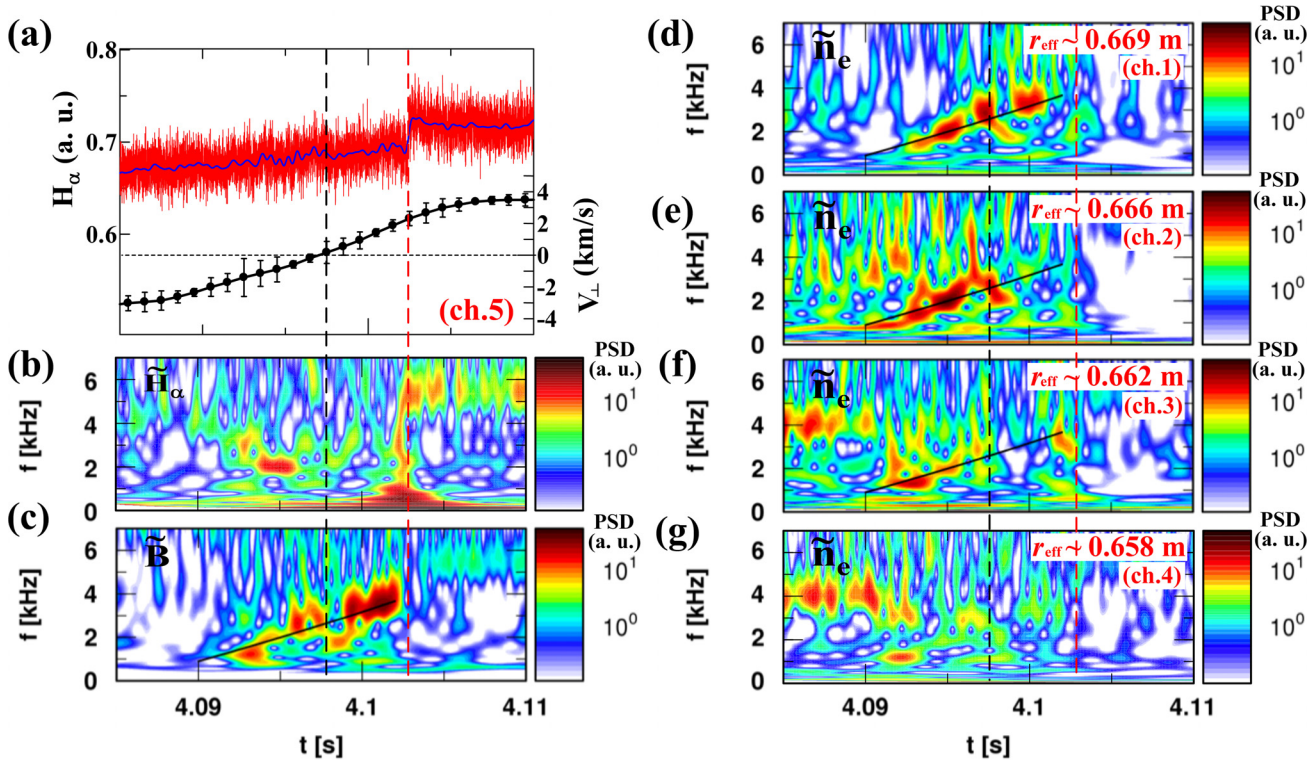


**FIG. 4.** Time evolutions of (a) $H_\alpha$ signal (the blue solid line indicates the fluctuations in the frequency band 0–2 kHz) and the perpendicular flow velocity $V_\perp$ of the Doppler reflectometer at $r_{eff} \simeq 0.654$ m (black mark), and the wavelet spectra with (b) $H_\alpha$ signal fluctuations, (c) the magnetic fluctuations, and with the reflectometer density fluctuations for (d) $r_{eff} \simeq 0.669$ m, (e) $r_{eff} \simeq 0.666$ m, (f) $r_{eff} \simeq 0.662$ m, and (g) $r_{eff} \simeq 0.658$ m as a function of frequency. The black solid lines (eye-guide) are estimated from the peak of the low-frequency fluctuations to the polynomial curve fitting process. The vertical black dashed line indicates the timing of the transition of $V_\perp$ from negative to positive values, and the vertical red dashed line indicates the timing of the rise in $H_\alpha$ signal.

at $r_{eff} \simeq 0.666$ m for the low-frequency fluctuations with $f \simeq 2$ kHz from time lag −1.2 ms to +1.2 ms. It is found that the low-frequency fluctuation is elongated in the edge plasmas ($t \simeq 4.095$ s), when the propagation velocity becomes approximately zero. The spatial structure of the outermost four channels for the low-frequency fluctuations is consistent with the observations of the outward propagation for the peak of the integral low-frequency amplitude, as shown in Fig. 5. On the other hand, the innermost four channels exhibited a strong cross correlation between the low-frequency fluctuations with $f \simeq 2$ kHz, although there was no observation of a coherent low-frequency fluctuation, which seems to propagate inwards. Since the cross correlation analysis is the measure of similarity by using the amplitude and the phase of the low-frequency fluctuations. In addition, it is considered likely that the fluctuations of the innermost four channels are influenced strongly by the background noise in the inner plasmas. Therefore, the results seem to indicate that the low-frequency fluctuations propagate in both directions (inward and outward) away from the excitation position of the low-frequency fluctuation.

## IV. DISCUSSION

We investigated several experimental shots in addition to the typical experimental shot (#118187) in order to understand the plasma parameter dependence on the dynamical response of the low-frequency density fluctuations in the edge region of LHD plasmas. The codirection tangential (∼6 MW) and the counterdirection tangential (∼4 MW) NBI powers are changed for the experimental shots #118178 and #118180. The power of tangential NBIs is the injected power. Figure 7 shows the temporal evolution of plasma parameters such as (a) the perpendicular flow velocity $V_\perp$ at $r_{eff} \simeq 0.654$ m, (b) the plasma current $I_P$, (c) the electron temperature gradient $\nabla T_e$, (d) the amplitude of the high-frequency density fluctuations with $f \simeq 30$–150 kHz, and (e) the low-frequency density fluctuations with $f \simeq 1$–3 kHz corresponding to the abrupt appearance of the density fluctuation with $f \simeq 2$ kHz in the edge region of LHD plasmas. It is found that neither the plasma current nor the electron temperature gradient shows a strong correlation with the abrupt burst of the low-frequency density fluctuation. On the other hand, at the onset of the low-frequency density fluctuation, the amplitude of high-frequency density fluctuations with $f \simeq 30$–150 kHz becomes approximately two times larger than the initial state before the tangential NBIs. In particular, in Figs. 7(a) and 7(e), the amplitude of density fluctuations with $f \simeq 2$ kHz becomes significantly stronger when the perpendicular flow velocity (i.e., radial electric field) approaches to zero within the experimental uncertainties (including the uncertainties on the measurement radial position). Therefore, it is considered likely that the amplitude of high-frequency fluctuation and the radial electric field have a strong correlation with the emerging of the low-frequency density fluctuation burst.

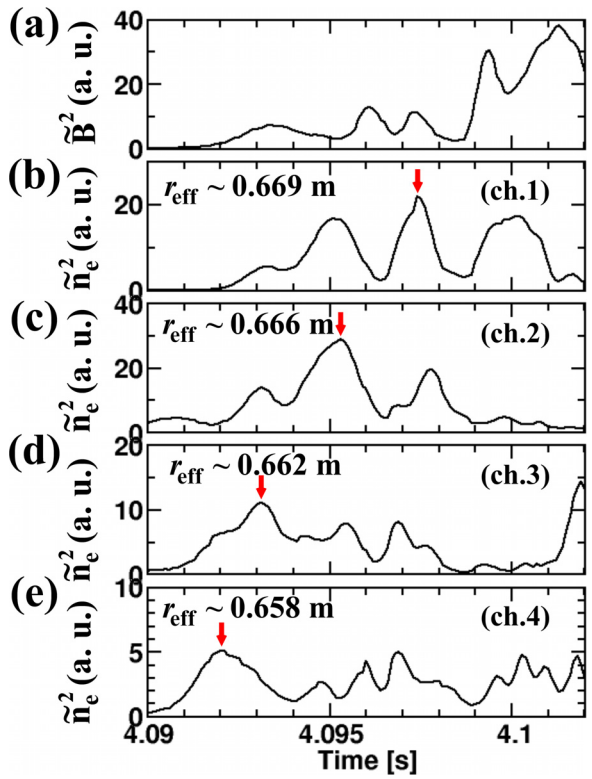


**FIG. 5.** Specific temporal evolution of the low-frequency fluctuation amplitudes with (a) the magnetic fluctuations, and (b)–(e) the density fluctuations at the poloidal flow velocity transition. The red arrows highlight the peak of the fluctuation envelope.

Finally, the theoretical predictions show that a low-frequency MHD mode can be excited via nonlinear interaction with turbulence,[4–7] and the decreasing of the radial electric field may be contributing to destabilize the low-frequency fluctuation in the vicinity of a magnetic island.[5,38] At the LCFS, the drift scale $\rho_s$ is approximately

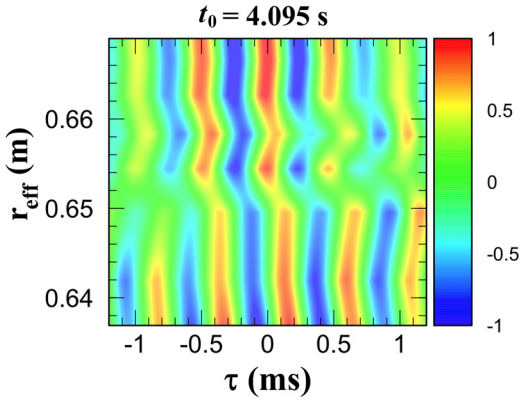


**FIG. 6.** Contours of cross correlation function of the Doppler reflectometer system channels with the reference channel at $r_{eff} \simeq 0.666$ m for the low-frequency fluctuations with $f \simeq 2$ kHz from time lag −1.2 ms to +1.2 ms. The red colors indicate a high level of cross correlation, whereas the blue colors indicate anticorrelation. The positive time delay means that the comparison channel comes after the reference.

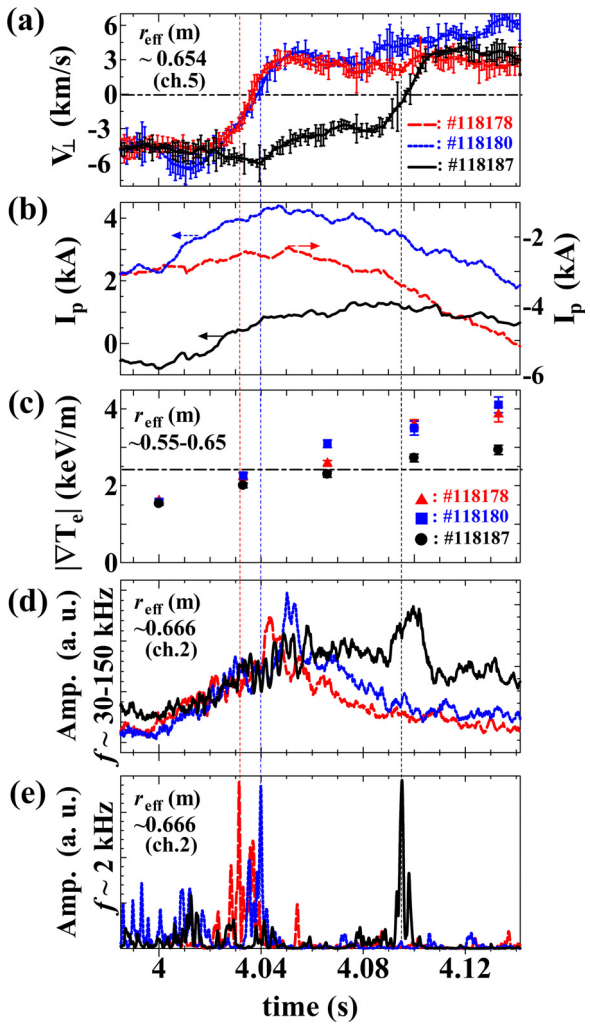


**FIG. 7.** Time evolutions of (a) the perpendicular flow velocity $V_\perp$ of the Doppler reflectometer at $r_{eff} \simeq 0.654$ m, (b) the plasma current $I_P$, (c) the electron temperature gradient $\nabla T_e$, (d) the amplitude of the high-frequency fluctuations with $f \simeq$ 30–150 kHz, and (e) the amplitude of the low-frequency fluctuations with $f \simeq 2$ kHz in the edge plasmas of LHD.

0.41 cm and the perpendicular wave number $k_\perp$ of the low-frequency fluctuation based on the poloidal number ($m \sim 2$) is approximately 0.02 $cm^{-1}$, which is in the range of $10^{-3} \lesssim k_\perp \rho_s < 0.1$ of the turbulence generated islands.[7] Therefore, it is considered likely that the low-frequency MHD mode[40] could be generated via nonlinear interaction with the high-frequency fluctuation when the radial electric field becomes approximately zero in the edge magnetic stochastic plasmas of LHD.

## V. CONCLUSIONS

The spatial response of low-frequency density fluctuation in the transition of the poloidal flow velocity ($V_\theta$) is investigated in the edge region of Large Helical Device (LHD) plasmas. The transition of the edge $V_\theta$ occurs by injecting the tangential NBIs, and consequently a

low-frequency (∼2 kHz) fluctuation is excited in the magnetic stochastic region. The low-frequency fluctuation feature is a chirping mode, and the main component of the mode is $m \sim 2$. In addition, the propagation velocity becomes approximately zero in the proximity of the appearance region of the low-frequency fluctuation, which is considered to be transmitted in both directions away from the excitation position. In particular, $H_\alpha$ signal shows a tiny increase concurrently with the disappearance of the low-frequency fluctuation. Therefore, it is considered that the low-frequency fluctuation has an impact on the edge transport in LHD. On the other hand, it is suspected that the low-frequency fluctuation is generated through nonlinear interaction with the high-frequency fluctuations when $V_\theta$ becomes approximately zero in edge plasma of LHD. However, the direct experimental evidence is insufficient to determine the phenomena; therefore, details of the verification will be investigated by using the other types of advanced fluctuation diagnostics (Beam Emission Spectroscopy, Electron Cyclotron Emission imaging) together in the future. Finally, these results will provide a better understanding of the dynamical response of low-frequency fluctuations at the transition of $V_\theta$ in the edge stochastic magnetic region of LHD.

## ACKNOWLEDGMENTS

We thank Professor S. Sakakibara, Professor U. Stroth, and Professor E. Wolfrum for strong support. The authors acknowledge all the members of LHD Experiment Group for their assistance. This work was partly supported by JSPS KAKENHI Grant Nos. 15H02336, 16H02442, 17H06089, and 19K23426. This work was also partly supported by the National Institute for Fusion Science grant administrative budgets (NIFS10ULHH021 and NIFS17KLPH030).

## REFERENCES

[1]R. Jiménez-Gómez, E. Ascasíbar, T. Estrada, I. García-Cortés, B. Van Milligen, A. López-Fraguas, I. Pastor, and D. López-Bruna, Fusion Sci. Technol. **51**, 20 (2007).
[2]K. Ida, S. Inagaki, Y. Suzuki, S. Sakakibara, T. Kobayashi, K. Itoh, H. Tsuchiya, C. Suzuki, M. Yoshinuma, Y. Narushima, M. Yokoyama, A. Shimizu, S.-I. Itoh, and LHD Experiment Group, New J. Phys. **15**, 013061 (2013).
[3]M. Kobayashi, S. Morita, C. F. Dong, Z. Y. Cui, Y. D. Pan, Y. D. Gao, H. Y. Zhou, Y. Feng, S. Masuzaki, M. Goto, T. Morisaki, H. Yamada, J. Cheng, P. Sun, Q. W. Yang, X. R. Duan, and LHD Experiment Group, Nucl. Fusion **53**, 033011 (2013).
[4]S.-I. Itoh, K. Itoh, and M. Yagi, Phys. Rev. Lett. **91**, 045003 (2003).
[5]F. L. Waelbroeck, F. Militello, R. Fitzpatrick, and W. Horton, Plasma Phys. Controlled Fusion **51**, 015015 (2009).
[6]O. Agullo, M. Muraglia, S. Benkadda, A. Poyé, N. Dubuit, X. Garbet, and A. Sen, Phys. Plasmas **24**, 042308 (2017).
[7]O. Agullo, M. Muraglia, S. Benkadda, A. Poyé, N. Dubuit, X. Garbet, and A. Sen, Phys. Plasmas **24**, 042309 (2017).
[8]F. Watanabe, K. Toi, S. Ohdachi, S. Takagi, S. Sakakibara, K. Y. Watanabe, S. Morita, K. Narihara, K. Tanaka, K. Yamazaki, and LHD Experimental Group, Plasma Phys. Controlled Fusion **48**, A201 (2006).
[9]F. Watanabe, K. Toi, S. Ohdachi, S. Sakakibara, S. Morita, K. Narihara, Y. Narushima, T. Morisaki, C. Suzuki, K. Tanaka, T. Tokuzawa, K. Y. Watanabe, and LHD Experimental Group, Nucl. Fusion **48**, 024010 (2008).
[10]R. Jiménez-Gómez, A. Könies, E. Ascasíbar, F. Castejón, T. Estrada, L. G. Eliseev, A. V. Melnikov, J. A. Jiménez, D. G. Pretty, D. Jiménez-Rey, M. A. Pedrosa, A. de Bustos, and S. Yamamoto, Nucl. Fusion **51**, 033001 (2011).
[11]Y. Takemura, S. Sakakibara, Y. Narushima, M. Okamoto, K. Y. Watanabe, Y. Suzuki, S. Ohdachi, K. Ida, M. Yoshinuma, K. Tanaka, T. Tokuzawa, K. Narihara, I. Yamada, H. Yamada, and LHD Experiment Group, Nucl. Fusion **52**, 102001 (2012).
[12]Y. Suzuki, K. Ida, K. Kamiya, M. Yoshinuma, H. Tsuchiya, S. Inagaki, S. Sakakibara, K. Y. Watanabe, Y. Narushima, S. Ohdachi, I. Yamada, R. Yasuhara, K. Tanaka, T. Akiyama, H. Yamada, and the LHD Experiment Group, Plasma Phys. Control. Fusion **55**, 124042 (2013).
[13]Y. Suzuki, K. Ida, K. Kamiya, M. Yoshinuma, H. Tsuchiya, M. Kobayashi, G. Kawamura, S. Ohdachi, S. Sakakibara, K. Y. Watanabe, S. Hudson, Y. Feng, I. Yamada, R. Yasuhara, K. Tanaka, T. Akiyama, T. Morisaki, and LHD Experiment Group, Nucl. Fusion **56**, 092002 (2016).
[14]J. L. Velasco, J. A. Alonso, I. Calvo, and J. Arévalo, Phys. Rev. Lett. **109**, 135003 (2012).
[15]C. Moon, K. Ida, T. Tokuzawa, K. Tanaka, M. Yoshinuma, T. Kobayashi, S. Inagaki, K. Itoh, and LHD Experiment Group, Plasma Fusion Res. **10**, 3402053 (2015).
[16]K. Ida, H. Yamada, H. Iguchi, K. Itoh, and CHS Group, Phys. Rev. Lett. **67**, 58 (1991).
[17]V. V. Bulanin, S. V. Lebedev, L. S. Levin, and V. S. Roytershteyn, Plasma Phys. Rep. **26**, 813 (2000).
[18]G. D. Conway, J. Schirmer, S. Klenge, W. Suttrop, E. Holzhauer, and ASDEX Upgrade Team, Plasma Phys. Controlled Fusion **46**, 951 (2004).
[19]G. D. Conway, C. Angioni, R. Dux, F. Ryter, A. G. Peeters, J. Schirmer, C. Troester, CFN Reflectometry Group, and ASDEX Upgrade Team, Nucl. Fusion **46**, S799 (2006).
[20]T. Happel, T. Estrada, E. Blanco, V. Tribaldos, A. Cappa, and A. Bustos Yuh, Rev. Sci. Instrum. **80**, 073502 (2009).
[21]P. Hennequin, C. Honoré, A. Truc, A. Quéméneur, and N. Lemoine, Rev. Sci. Instrum. **75**, 3881 (2004).
[22]P. Hennequin, P. Hennequin, C. Honoré, A. Truc, A. Quéméneur, C. Fenzi-Bonizec, C. Bourdelle, X. Garbet, G. T. Hoang, and Tore Supra Team, Nucl. Fusion **46**, S771 (2006).
[23]J. C. Hillesheim, W. A. Peebles, T. L. Rhodes, L. Schmitz, T. A. Carter, P.-A. Gourdain, and G. Wang, Rev. Sci. Instrum. **80**, 083507 (2009).
[24]J. C. Hillesheim, W. A. Peebles, T. L. Rhodes, L. Schmitz, A. E. White, and T. A. Carter, Rev. Sci. Instrum. **81**, 10D907 (2010).
[25]M. Hirsch, E. Holzhauer, J. Baldzuhn, B. Kurzan, and B. Scott, Plasma Phys. Controlled Fusion **43**, 1641 (2001).
[26]N. Oyama, H. Takenaga, T. Suzuki, Y. Sakamoto, A. Isayama, and JT-60 Team, Plasma Fusion Res. **6**, 1402014 (2011).
[27]W. A. Peebles, T. L. Rhodes, J. C. Hillesheim, L. Zeng, and C. Wannberg, Rev. Sci. Instrum. **81**, 10D902 (2010).
[28]J. Schirmer, G. D. Conway, E. Holzhauer, W. Suttrop, H. Zohm, and ASDEX Upgrade Team, Plasma Phys. Controlled Fusion **49**, 1019 (2007).
[29]T. Tokuzawa, A. Ejiri, K. Kawahata, K. Tanaka, I. Yamada, M. Yoshinuma, K. Ida, and C. Suzuki, Rev. Sci. Instrum. **83**, 10E322 (2012).
[30]T. Tokuzawa, S. Inagaki, A. Ejiri, R. Soga, I. Yamada, S. Kubo, M. Yoshinuma, K. Ida, C. Suzuki, K. Tanaka, T. Akiyama, N. Kasuya, K. Itoh, K. Watanabe, H. Yamada, K. Kawahata, and LHD Experiment Group, Plasma Fusion Res. **9**, 1402149 (2014).
[31]I. Yamada, K. Narihara, H. Funaba, H. Hayashi, and LHD Experimental Group, Rev. Sci. Instrum. **75**, 3912 (2004).
[32]K. Ida, S. Kado, and Y. Liang, Rev. Sci. Instrum. **71**, 2360 (2000).
[33]M. Yoshinuma, K. Ida, M. Yokoyama, M. Osakabe, and K. Nagaoka, Fusion Sci. Technol. **58**, 375 (2010).
[34]K. Ida, K. Kondo, K. Nagasaki, T. Hamada, S. Hidekuma, F. Sano, H. Zushi, T. Mizuuchi, H. Okada, S. Besshou, H. Funaba, K. Watanabe, and T. Obik, Phys. Rev. Lett. **76**, 1268 (1996).
[35]K. Kamiya, K. Ida, M. Yoshinuma, C. Suzuki, Y. Suzuki, M. Yokoyama, and LHD Experiment Group, Nucl. Fusion **53**, 013003 (2013).
[36]C. Moon, M. Yoshinuma, M. Emoto, and K. Ida, Fusion Eng. Des. **104**, 56 (2016).
[37]S. Sakakibara, H. Yamada, and LHD Experiment Group, Fusion Sci. Technol. **58**, 471 (2010).
[38]K. C. Shaing, Phys. Plasmas **9**(8), 3470 (2002).
[39]A. J. Creely, K. Ida, M. Yoshinuma, T. Tokuzawa, T. Tsujimura, T. Akiyama, R. Sakamoto, M. Emoto, K. Tanaka, and C. A. Michael, Rev. Sci. Instrum. **88**, 073509 (2017).
[40]S. Sakakibara, K. Y. Watanabe, S. Ohdachi, Y. Narushima, K. Toi, K. Tanaka, K. Narihara, K. Ida, T. Tokuzawa, K. Kawahata, H. Yamada, A. Komori, and LHD Experiment Group, Fusion Sci. Technol. **58**, 176 (2010).